Thermal Design Consideration of Medium Voltage High Frequency Transformers

Haoming Wang*†, Zhichen Guo*, S. Milad Tayebi*, Xin Zhao*, Qingyun Huang*, Ruiyang Yu*, Qingxin Yang†, Yongjian Li†, Alex Q. Huang*
Email: hmwang@utexas.edu
*Department of Electrical and Computer EngineeringSemiconductor Power Electronics Center, University of Texas at Austin, Austin, USA
†State Key Laboratory of Reliability and Intelligence of Electrical Equipment, Hebei University of Technology, Tianjin, CHN

***Abstract*—This paper describes a thermal design using epoxy potting for high frequency transformer (HFT) for medium voltage high power electronic applications, namely emerging solid-state transformers. To address HFT's thermal stress problem, thermal performance of the HFT with air and epoxy potting cooling method are both simulated by magneto-thermal-fluid coupling method (MTFCM). The effectiveness of the simulation analysis is verified in a 100 kW DC-DC resonant converter. Influencing factors including distance between the high frequency transformer and the metal enclosure, epoxy thermal conductivity and heat sink placements are simulated and analyzed. Finally, an optimal cooling structure is proposed for future high power HFTs.**

Keywords—HFT, MTFCM, thermal, epoxy potting, heat sink

NOMENCLATURE

J_e	Eddy current density.
T	Vector potential.
Ω	Magnetic scalar potential.
J	Current density.
σ	Electric conductivity.
E	Electric field strength.
μ	Magnetic permeability.
B	Magnetic flux density.
J_s	Source current density.
H_s	Magnetic field in an infinite space generated by source current.
r	Diameter of winding.
P_h	Hysteresis loss density.
k_i	Steinmetz coefficient.
K, α, β	Original steinmetz coefficient.
f	Switching frequency.
B_m	Maximum magnetic flux density.
D	Duty cycle.
W_c	Hysteresis loss.
$P_h^{(i)}$	Hysteresis loss density per unit.
$V^{(i)}$	Volume of each unit.
ρ_m	Material density.
k_{cu}	Copper filling factor.
d_r	Litz wire strand diameter.
ω_ω	Width of each winding layer.
R_{ac}	AC resistance of the winding.
R_{dc}	DC resistance of the winding.
$K_{ac/dc}$	Ac/dc resistance ratio.
q	Loss density.
W	Loss of heat source.
V	Equivalent volume.
ρ	Air density.
t	Time.
g	Acceleration of gravity.
U	Velocity vector of fluid.
u, v, w	x, y, z components of U, respectively.
μ_r	Dynamic viscosity coefficient.
C_p	Specific heat capacity of the fluid.
T_i	Unit temperature.
λ	Thermal conductivity of the fluid.

I. INTRODUCTION

Aiming at replacing century-old line frequency transformer (LFT), the Solid-State Transformer (SST) has been investigated intensively in the past decade due to its ability to offer many smart functionalities such as voltage regulation and power flow control in the distribution power grid [1-3]. The HFT plays an important role in the SST to provide galvanic isolation and necessary voltage conversion ratio to match the input and output voltages. Thanks to the use of emerging power devices such as SiC MPOSFET, the power level and switching frequency of the HFT is also increasing, resulting in improved power density [4-5].

Nevertheless, a high power HFT with a substantially reduced size has many extra challenges. First, the typical operational square voltage waveform and non-sinusoidal current has a major effect on the core and winding losses. Moreover, how to design and trade-off the HFT capacitance, leakage and magnetizing inductance, and the operating magnetic flux density has no definitive guidelines. Furthermore, due to small size and high power density of HFT, the thermal performance of high power HFTs becomes a major limiting factor in the overall SiC converter [6-8].

The thermal challenge is a direct result of extremely poor thermal dissipation path in high density HFTs. The distance between the inner and outer windings, inner winding and the bobbing, the bobbing and the core are so small and compact, the generated heat from these regions are not easy to dissipate. To address this problem, an enhanced cooling concept based on extra high thermal conductivity aluminum parts to transfer the heat from the core and winding surface to a water-cooled heat sink is proposed in [9]. Recently, a thermal model based on detailed steady-state thermal network models consisting of conduction, convection, and radiation thermal resistances is presented in [10].

In this paper, the enhanced thermal performance of a high power HFT with epoxy potting is analyzed with the help of simulation. Section II describes the MTFCM for HFT thermal simulation, which is used to analyze air and epoxy potting cooling performance. Section III presents the thermal performance simulation results of air cooling method, and the verification for the MTFCM. A new epoxy potting cooling method is introduced in Section IV, and its thermal

978-1-7281-4829-8/20/$31.00 ©2020 IEEE

performance is analyzed systematically. Losses induced in the aluminum metal enclosure is calculated. Other factors affecting the HFT's thermal performance including distance between the HFT and the metal box, thermal conductivity of the epoxy, and heat sink placements are also studied. Finally, Section V provides a discussion and summary of main contributions.

II. MTFCM CALCULAITON MODEL

A multi-physic model is developed to simulate the internal temperature distribution [11]. The MTFCM (magneto-thermal-fluid coupling method) simulation process is shown in Fig. 1.

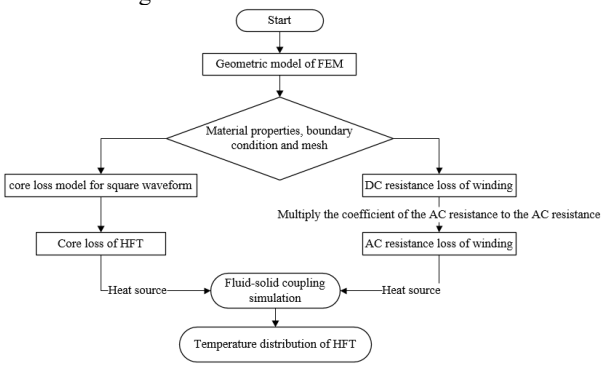

Fig. 1. Simulation process of temperature distribution

A. 3D Field-Circuit Coupling Calculation model

The commercial software Infolytica MagNet based on T-Ω method [12] is used to calculate HFT core loss. The advantages of this method include less unknown variables, simpler numerical calculation, shorter calculation time and smaller computer resources. The mathematical basis of the T-Ω method is described below. In the Eddy current region, the vector potential is defined as follows:

$$J_e = \nabla \times T \tag{1}$$

where, J_e is the eddy current density, T is the vector potential. The first equation of the Maxwell Equations can be written as:

$$\nabla \times \left(H - T \right) = 0 \tag{2}$$

Therefore,

$$H = T - \nabla \Omega \tag{3}$$

Based on the constitutive relationship:

$$J = \sigma E \tag{4}$$

and ignore the displacement current in the conductor, equation (4) can be transformed to

$$E = \frac{1}{\sigma} \nabla \cdot T \tag{5}$$

The control equation in the Eddy current region is

$$\nabla \times \frac{1}{\sigma} \nabla \times T + \frac{\partial}{\partial t} \mu \left(T - \nabla \Omega \right) = 0 \tag{6}$$

For a nodal element, the Coulomb criterion is adopted, and a penalty function term is introduced

$$-\nabla \frac{1}{\sigma} \nabla \cdot T \tag{7}$$

Then,

$$\nabla \times \frac{1}{\sigma} \nabla \times T - \nabla \frac{1}{\sigma} \nabla \cdot T + \frac{\partial}{\partial t} \mu \left(T - \nabla \Omega \right) = 0 \tag{8}$$

Applying $\nabla \cdot B = 0$,

$$\nabla \cdot \left[\mu \left(T - \nabla \Omega \right) \right] = 0 \tag{9}$$

The first equation of Maxwell's equations in the non-eddy current region is:

$$\nabla \times H = J_s \tag{10}$$

So it is not necessary to introduce a vector potential in this region. Then, the formula for calculating the magnetic field strength is as follows:

$$H = H_s - \nabla \Omega \tag{11}$$

Where, H_s needs to be calculated according to Biot-Savart Law:

$$H_s = \frac{1}{4\pi} \int_{\Omega} \frac{J_s \times r}{r^3} d\Omega \tag{12}$$

The control equation in the non-eddy current region is:

$$\nabla \cdot \left[\mu \left(-\nabla \Omega + H_s \right) \right] = 0 \tag{13}$$

For the HFT case under study, the transformer voltage is a square waveform with a duty cycle of 0.5. According to [9], a simple core loss model for square wave excitation is presented as follows

$$P_h = 2^{\alpha+\beta} k_i f^{\alpha} B_m^{\beta} D^{1-\alpha} \tag{14}$$

where, $k_i = \dfrac{K}{2^{\beta-1} \pi^{\alpha-1} \left(0.2761 + \dfrac{1.7061}{\alpha + 1.354} \right)}$ is the Steinmetz coefficient.

The core loss W_c is obtained by calculating P_h corresponding to maximum flux density B_m on each unit:

$$W_c = \sum_{i=1}^{N} P_h^{(i)} \rho_m V^{(i)} \tag{15}$$

The DC resistance loss calculated by the finite element simulation multiplied by the AC-DC coefficient $K_{ac/dc}$ is the total winding loss. $K_{ac/dc}$ can be used [10]:

$$K_{ac/dc} = \frac{R_{ac}}{R_{dc}} \approx 1 + \frac{1}{12} \left(\pi f \sigma \mu k_{\mathrm{cu}} \omega_{\omega} d_r \right)^2 \tag{16}$$

C-core type nanocrystalline core loss is first calculated by the FEA method. Fig. 2. shows the calculated eddy current loss on the core surface with different HFT leakage inductance at 100A rms input current. As seen in the Fig. 2, as the leakage inductance increases, the eddy current loss on nanocrystalline core surface also increases linearly. Since the

nanocrystalline core is sensitive to magnetic flux leakage, the smaller the leakage inductance, the better the winding structure. However, the difficulty for winding fabrication should be considered. The final HFT winding structure used in this paper is shown in Fig. 3. The leakage inductance is 2.11 μH. The external circuit in Field-Circuit Coupling Calculation model [13] under short circuit condition is given in Fig. 4.

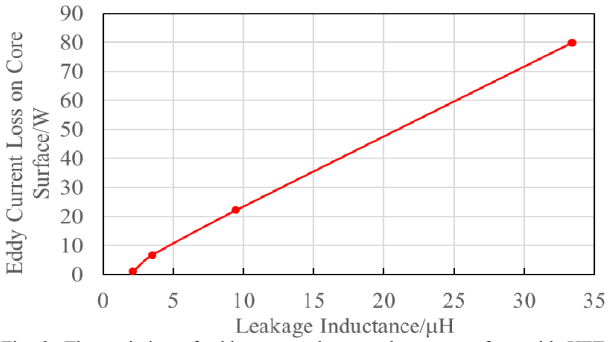

Fig. 2. The variation of eddy current loss on the core surface with HFT leakage inductance at 100A rms input current

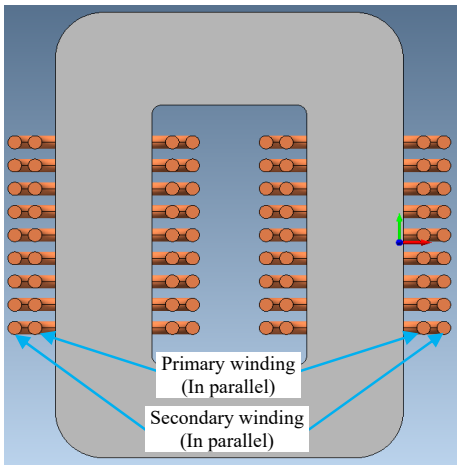

Fig. 3. HFT winding structure

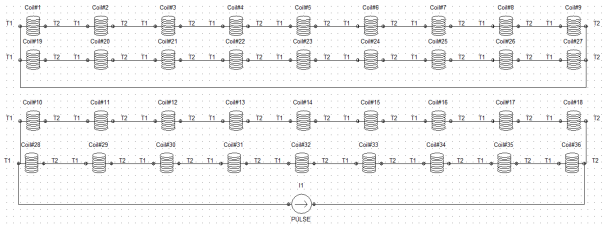

Fig. 4. The external circuit in Field-Circuit Coupling Calculation model under short circuit condition

B. 3D Fluid-Solid Coupling Calculation Model

HFT core and winding losses are treated as heat source. In this case, the heat sources are considered to be uniform. Loss density q is therefore

$$q = \frac{W}{V} \tag{17}$$

According to the heat transfer and fluid dynamics analysis of the HFT thermal model, the heat dissipation process mainly includes the heat conduction between the core, winding and bobbing, heat transfer between the core, winding and bobbing surface and the air. Since the thermal radiation effect in this calculation model is small, it can be ignored. The control equation for the fluid-solid coupling calculation can be described as

Continuity equation:

$$\frac{\partial(\rho)}{\partial t}+\frac{\partial(\rho u)}{\partial x}+\frac{\partial(\rho v)}{\partial y}+\frac{\partial(\rho w)}{\partial z}=0 \tag{18}$$

Momentum equation:

$$\begin{cases}\dfrac{\partial(\rho u)}{\partial t}+\nabla\cdot(\rho u U)=-\dfrac{\partial \rho}{\partial x}+\mu_r\Delta u\\ \dfrac{\partial(\rho v)}{\partial t}+\nabla\cdot(\rho v U)=-\dfrac{\partial \rho}{\partial y}+\mu_r\Delta v\\ \dfrac{\partial(\rho w)}{\partial t}+\nabla\cdot(\rho w U)=-\dfrac{\partial \rho}{\partial z}+\mu_r\Delta w-\rho g\end{cases} \tag{19}$$

Energy equation:

$$\frac{\partial(\rho T_i)}{\partial t}+\frac{\partial(\rho u T_i)}{\partial x}+\frac{\partial(\rho v T_i)}{\partial y}+\frac{\partial(\rho w T_i)}{\partial z}=\frac{\lambda}{C_p}\Delta T_i \tag{20}$$

III. HFT Temperature Distribution Simulation Result and Varivification

A. HFT Temperature Simulation Results with Air cooling

To cool the HFT, the most common way is the forced air cooling with a fan. The cooling performance of the fan is shown in Fig. 5, the size of fan is the same as the core window area. It can be seen the hot spot temperature of core and winding will decrease as the applied air velocity increases. However, when the velocity reaches a certain value (3.5 m/s), increasing velocity can no longer improve the cooling effect, and the hot spot temperature of core and winding keep steady at 113 ℃ and 108 ℃. Therefore, only using fans for cooling is not enough for high power medium voltage HFT.

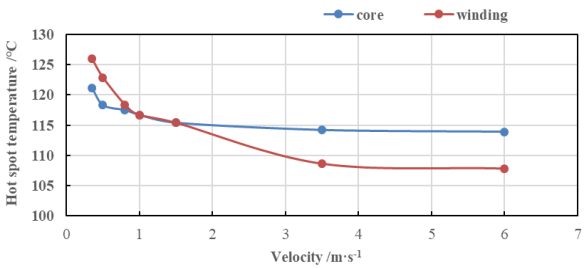

Fig. 5. Hot spot temperature of the HFT with different fan air velocity

B. Experimental Results and Verification

The test configuration is a half bridge DC-DC resonant converter using back-back connection, and the schematic and HFT input voltage and current waveform are given in Fig. 6. Fig. 7 shows the hardware under test. The converter utilized 1.7 kV SiC MOSFET modules from Wolfspeed. In the test,

the HFT input voltage rms value is 589 V and the rms value of the HFT current is 169 A, and the frequency is 16.5 kHz. The leakage inductance value calculated by the magnetic field energy method is 2.02 μH, and the tested value is 2.11 μH. The error is less than 5%, which verifies the validity of the magnetic field calculation. The calculated core and winding loss is 112W and 135W, respectively, which are treated as heat sources in the thermal simulation. Fig. 7 is the thermal simulation result and Fig. 8 is the thermal test result. The simulation and experimental temperature error is less than 5%, which verifies the effectiveness of the MTFCM.

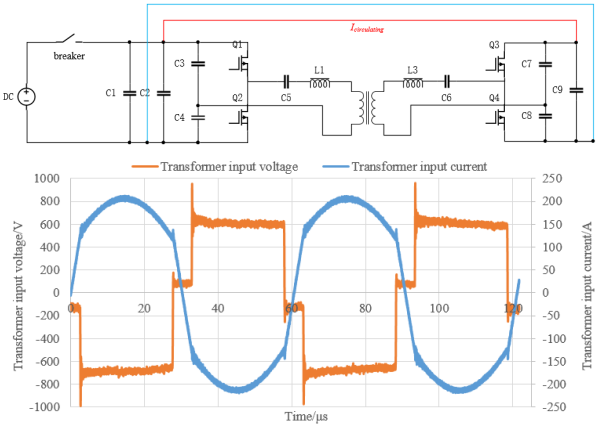

Fig. 6. Schematic of test system and HFT test input waveform

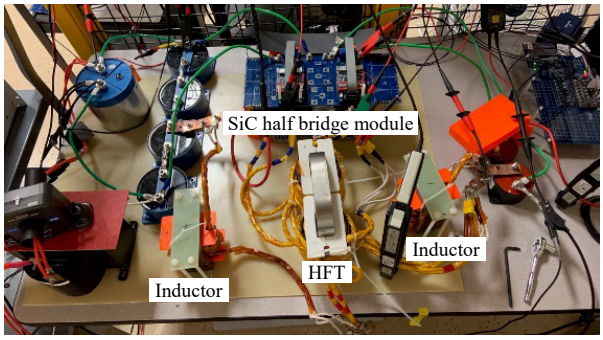

Fig. 7. Hardware implementation of test

(a)

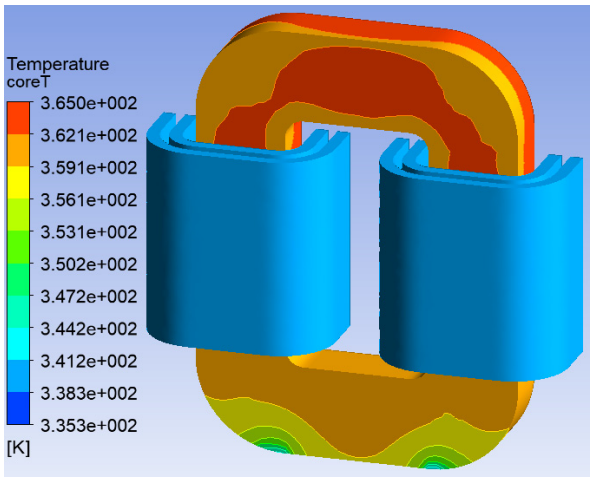

(b)

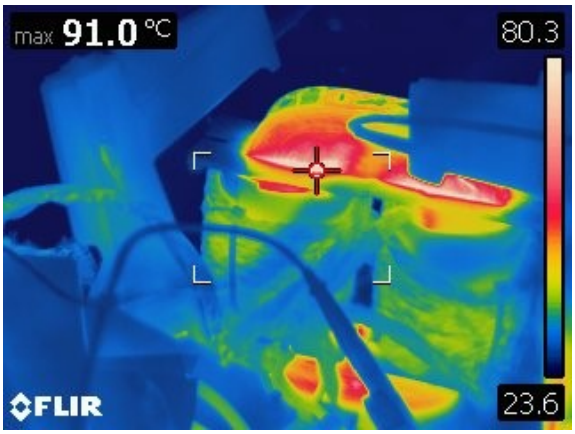

Fig. 8. Comparison of HFT temperature distribution between simulation and experiment under 100kW

IV. Design and Simulation of HFT with Epoxy Potting and Heat Sinks

A. HFT Thermal Structure with Epoxy Potting and Heat Sinks

Aiming at improving the thermal performance of the HFT, a new cooling method is proposed by potting the whole HFT with higher thermal conductivity epoxy. Several factors are considered in designing such a cooling structure, including the distance between the HFT and the metal enclosure, extra losses on the metal enclosure and the placement of the heatsink. Epoxy with proper thermal conductivity should be selected. Base on the core size under study, the type of heat sink is selected. Table I summaries the HFT specifications and the structure of HFT with epoxy potting is given in Fig. 9.

TABLE I. HFT Specifications

Position	Size
FINMET Core	180 mm×30 mm×240 mm
Winding	9 turns, 3×1650×0.1 mm
Heat sink	200 mm×240 mm×83 mm

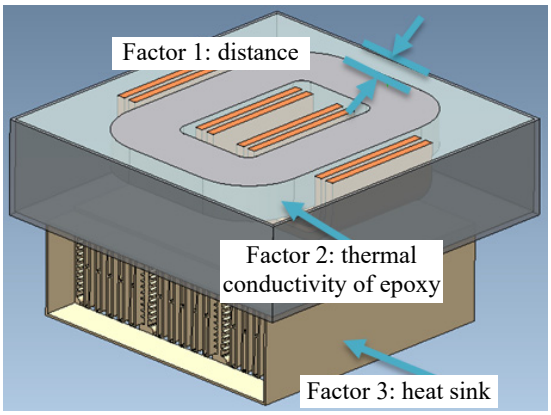

Fig. 9. The structure of HFT with epoxy potting

B. *Simulation Results Based on Magneto-Thermal-Fluid Coupling Method*

In the simulation, the rms value of the applied voltage and current are 1.3 kV and 308 A respectively, and the frequency is 16.5 kHz. The calculation value of core and winding loss are 352 W and 449 W. Then the temperature distribution is simulated by using these losses as the heat source. To determine the best distance between the HFT and the metal box, the eddy current loss of the metal box and temperature distribution are simulated as the distance changes. The result is shown in Fig. 10. With the distance increasing, the hot spot temperature will increase and the loss of metal box will decrease. According to these simulation results, the best distance should be around 7 mm. At this distance, the loss of metal box is only 7.5 W and the hot spot temperature of HFT is 84 ℃.

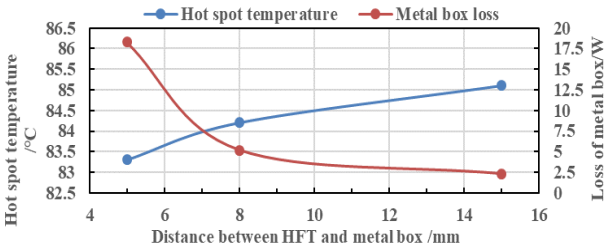

Fig. 10. HFT hot spot temperature and loss of metal box with different distance between HFT and metal box

Then the distance between the HFT and metal box is fixed at 7 mm, the thermal conductivity of epoxy is changed from 0.2 $W \cdot m^{-1} \cdot K^{-1}$ to 3.9 $W \cdot m^{-1} \cdot K^{-1}$. As can be seen from Fig. 11, the hot spot temperature will decrease as thermal conductivity of epoxy increases. But the trend of hot spot temperature reduction is gradually slowing down. Based on the simulation and economic considerations, epoxy of 1.7 $W \cdot m^{-1} \cdot K^{-1}$ thermal conductivity is chosen.

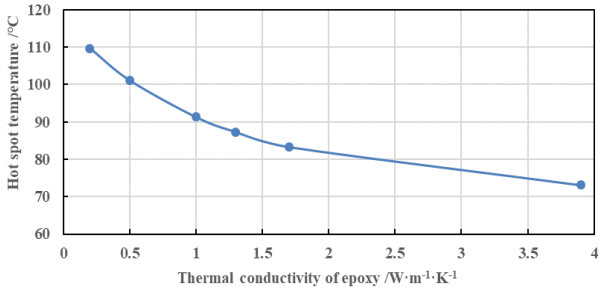

Fig. 11. HFT hot spot temperature with different epoxy thermal conductivity

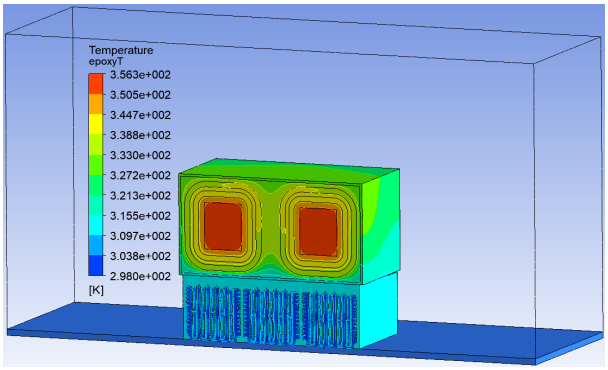

Fig. 12. Temperature distribution of HFT with 1 heat sink (optimal cooling structure)

Finally, the influence of number of heat sinks on the temperature rise is simulated. Added one extra heat sink (total two heatsink) only reduces the hot spot temperature by 5 ℃. From the above calculation and analysis, the optimal cooling structure of the transformer is the distance between HFT and metal box is 7 mm, thermal conductivity of epoxy is 1.7 $W \cdot m^{-1} \cdot K^{-1}$, and only one heat sink is used. Compared with HFT with fan cooling method, the hot spot temperature in this design will drop by 31.7 ℃ as displayed in Fig. 12.

V. Conclusions

This paper presents a thermal simulation study of a high power HFT. Firstly, the MTFCM is used for thermal calculation and its correctness is verified by a HFT prototype tested under 100 kW, 16.5 kHz condition. The temperature error between the measurement and simulation is less than 5%. The same method is then applied to evaluate the performance of epoxy potted HFT. Finally, the predicted hot spot temperature will decrease from 114 ℃ to 83.3 ℃ compared to standard air cooling method.

Acknowledgment

This work is primarily supported by the DOE SunShot program under contract number DE-EE0008348. The first author is supported by the Joint Doctoral Training Foundation of HEBUT under Grant 2018HW0003.

References

[1] X. She, A. Q. Huang, R. Burgos, "Review of Solid-State Transformer Technologies and Their Application in Power Distribution Systems," IEEE Journal of Emerging and Selected Topics in Power Electronics, vol. 1, no. 3, pp. 186-198, Spet. 2013.

[2] A. Q. Huang, "Medium-Voltage Solid-State Transformer: Technology for a Smarter and Resilient Grid," IEEE Industrial Electronics Magazine, vol. 10, no. 3, pp. 29-42, Spet. 2016.

[3] J. Huber, J. W. Kolar, "Solid-State Transformers: On the Origins and Evolution of Key Concepts," IEEE Industrial Electronics Magazine, pp. 19-28, 2016.

[4] J. Huber, G. Ortiz, F. Krismer, N. Widmer, and J. W. Kolar, "η-ρ Paretooptimization of bidirectional half-cycle discontinuous-conduction-modeseries-resonant DC/DC converter with fixed voltage transfer ratio," inProc. IEEE Appl. Power Electron. Conf. Expo. (APEC), Long Beach,CA, USA, Mar. 2013, pp. 1413–1420.

[5] M. Mogorovic and D. Dujic, "Medium frequency transformer leakage inductance modeling and experimental verification," in Proc. IEEE EnergyConvers. Congr. Expo., 2017, pp. 419–424.

[6] D. Hou, et al, "New High-Frequency Core Loss Measurement Method With Partial Cancellation Concept," IEEE Transactions on Power Electronics, vol. 32, no. 4, pp. 2987-2994, 2017.

[7] M. Mu , Q. Li , D. J. Gilham , et al, "New Core Loss Measurement Method for High-Frequency Magnetic Materials," IEEE Transactions on Power Electronics, vol. 29, no. 8, pp. 4374-4381, 2014.

[8] M. Mogorovic, D. Dujic, "Sensitivity Analysis of Medium-Frequency Transformer Designs for Solid-State Transformers," IEEE Transactions on Power Electronics, vol. 34, no. 9, pp. 8356-8367, 2019.

[9] M. Mogorovic, D. Dujic, "100kW, 10kHz Medium Frequency Transformer Design Optimization and Experimental Verification," IEEE Transactions on Power Electronics, pp. 1-1, 2018.

[10] L. Michael, G. Ortiz, J. W. Kolar, "Design and Experimental Analysis of a Medium Frequency Transformer for Solid-State Transformer Applications," IEEE Journal of Emerging & Selected Topics in Power Electronics, pp. 110-123, 2016.

[11] H. Wang, Q. Yang, Y. Li, et al, "Numerical Calculation and Experimental Verification for Leakage Magnetic Field and Temperature Rise of Transformer Core Tie-Plate," IEEE Transactions on Applied Superconductivity, vol. 29, no. 2, pp. 1-1, 2019.

[12] Z. Cheng and N. Takahashi, Electromagnetic and Thermal Field Modeling and Application in Electrical Engineering, 1st ed. Beijing, China:Science Press, 2009.

[13] H. Wang, Q. Yang, Y. Li, et al, "Electromagnetic Characteristic Calculation of Several Parallel Coils for High Current Transformer Based on Field-Circuit Coupling Method," IEEE Transactions on Applied Superconductivity, vol. 29, no. 2, pp. 1-1, 2019.